Brief summary of latest experimental results with a mass-flow calorimetry system for anomalous heat effect of nano-composite metals under D(H)-gas charging

A. Kitamura[1,2,*], A. Takahashi[1,3], R. Seto[1], Y. Fujita[1], A. Taniike[2] and Y. Furuyama[2]

[1]Technova Inc., Tokyo 1000011, Japan
[2]Graduate School of Maritime Sciences, Kobe University, Kobe 6580022, Japan
[3]Osaka University, Suita 5650871, Japan

A mass-flow calorimetry system has been installed to investigate the excess power phenomenon at elevated temperatures. The first trial runs with a silica-included Cu·Ni nano-composite sample (CNS) containing 4.1 g of Ni showed an implication of a few days lasting excess power of 5 W/g-Ni. Next, a Cu·Ni·Zr oxide nano-composite sample (CNZ4) containing 61 g of Ni has been examined to show excess power of 15 W lasting for 3 days and gradually increasing at a rate of 10 W per 3 weeks. Each corresponds to 30 eV/atom-Ni and 100 eV/atom-Ni, implying a nuclear origin of the excess energy.

Keywords: Cu·Ni·ZrO$_2$, Cu·Ni·SiO$_2$, excess, oil-cooling, 30–100 eV/atom-Ni.

Introduction

THERE has been increasing interest in hydrogen gas-charged Ni-based samples for excess energy generation owing to broader accessibility of nickel than palladium (Pd). One successful work using a Ni·Cu·Mn alloy thin wire has been published recently[1]. In addition, a number of entrepreneurs are publicizing their own 'products' on websites with undisclosed details[2–4], although some of them are open to dispute.

We have been studying the phenomenon of anomalous heat evolution from hydrogen isotope-loaded nano-composite samples at elevated temperatures as well as room temperature using an A_1A_2 twin H(D)-absorption and calorimetry system[5,6], which was first used for Pd samples to find the size effect on the absorption characteristics of Pd powder[7]. Recent experiments have utilized Ni-based nano-composite samples supported by zirconia, Pd_1Ni_7/ZrO_2 ('PNZ'), Ni/ZrO_2 ('NZ'), $Cu_{0.081}Ni_{0.36}/ZrO_2$ ('CNZ'), $Cu_{0.21}Ni_{0.21}/ZrO_2$ ('CNZ2'), $Cu_{0.076}Ni_{0.36}/ZrO_2$ ('CNZ4') and a Ni-based nano-composite sample supported by silica, $Cu_{0.007}Ni_{0.03}/SiO_2$ ('CNS'). The results have been presented in the Annual Meetings of the Japan CF-Research Society (JCF) and International Conferences on Condensed Matter Nuclear Science (ICCF) – JCF12, ICCF17, JCF13, ICCF18 and JCF14. These have been/will be published soon[8–12] respectively.

The results from the ZiO$_2$-supported materials, PNZ, NZ, CNZ and CNZ2, are summarized, and the time-dependent data are re-analysed in a paper by Takahashi[13] for speculating a mechanism for heat release during the several weeks-lasting phase of D(H)-loading into the nano-composite samples. Several interesting features are involved: burst-like heat release with anomalously large values of differential heat of sorption (η) reaching about 600 eV/atom-H; large values of integrated heat reaching about 800 eV/atom-Ni from the CNZ sample absorbing (and weakly releasing) H, and abrupt large desorption with absorbed energy of 50–80 eV/atom-Ni observed almost exclusively in the first 573 K run for each sample.

To confirm the interesting phenomena, repeated measurements with improved signal-to-noise ratio, especially in calorimetry, are required. An improved H-absorption experimental system, C_1, having a reaction chamber (RC) with ten times larger volume and capable of mass-flow calorimetry using an oil coolant with a boiling point of 390°C, has been fabricated for this purpose. It has been applied first to the CNS sample[11], and then to the CNZ4 sample[12].

In the present article, we briefly review repeated anomalous heat evolution from the CNS and the CNZ4 samples using the C_1 system.

Description of the C_1 system

A schematic of the C_1 system named after the modification is shown in Figure 1. The system has a RC with a capacity of 500 cm^3, and a flow-calorimetry system

---

*For correspondence. (e-mail: kitamuraakira3@gmail.com)

capable of working at elevated temperatures up to 300°C with use of an oil coolant. On the outer surface of the RC, a coolant pipe and a 1 kW sheath heater (#1) are spirally wound alternately for heat removal and sample heating respectively. These are enclosed by a thin sheet of stainless steel for the purpose of thermal shield and close contact of the sheath heater to the side surface of the RC. All of these are supported by a stainless-steel pipe feeding H_2 gas to the sample in the RC, and surrounded again by a thermal shield made of ceramic fibre (Isowool 14C; Isolite Insulating Products Co. Ltd) not only on the side, but also at the top and bottom. The power to the heater is fed from a finely regulated DC power supply in a constant-current mode.

The coolant oil is an aromatic hydrocarbon (Barreltherm-400 (BT400); Matsumura Oil Co. Ltd), which has a boiling point of 390°C and practically usable maximum temperature of 330°C. The coolant is driven by a digital liquid tubing pump (Masterflex peristaltic pump) with a constant flow rate of 20 or 10 cm^3/min in the present work. Material of the plastic tube in the squeezing section is either Tygon or Viton. The coolant is fed to the RC from the bottom, and heated by the heater and the H-absorbing sample. After emerging from the top flange, the oil flows to an external heat exchanger of water chiller, set up outside the air temperature-regulated cabin, and cooled down to the ambient temperature, and fed back to the tubing pump through a water bath kept at a temperature of 24.0° ± 0.1°C (during summer) or 20.0° ± 0.1°C (during winter).

Seven thermocouples (TCs) are deployed; five points on the surface of the coolant pipe – TC1, TC2, TC3, TC5 and TC6; one point on the gas feed pipe – TC4, and TC0 for monitoring the ambient temperature. For flow-calorimetry measure, the difference in temperatures between TC2 just at the outlet from the RC for the outlet oil temperature and TC6 for the inlet oil temperature is used.

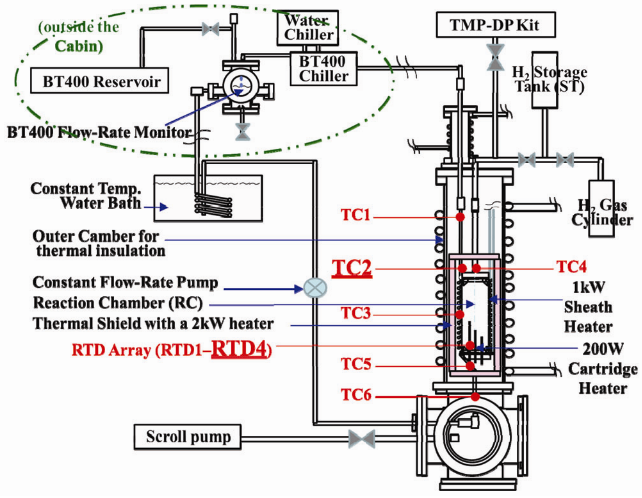

Figure 1. Schematic of the C_1 absorption system after modification of the flow rate monitor and addition of the 200 W cartridge heater.

In addition to the TCs, four resistance temperature detectors (RTDs) are deployed inside the RC to directly measure the sample temperature. The positions in the RC expressed as [radial position (mm), height (mm) from the bottom flange] are [10, 30], [0, 60], [10, 60] and [10, 90] respectively, for RTD1, RTD2, RTD3 and RTD4, in the earliest stage of the experiments for the sample CNS. Later for the sample CNZ4, the bottom flange was replaced by another with the RCs distributed at [10, 30], [10, 60], [10, 90] and [10, 120] respectively, to accommodate an additional 200 W cartridge heater (#2 heater) on the axis of the RC.

At the same time with this improvement, the coolant loop was also improved to enable monitoring the flow rate of the BT400 by counting the free-falling droplets of the BT400.

The amount of H atom absorbed in the sample is deduced from decrease in the number of H_2 molecules calculated from pressure values at the storage tank (ST), P_s, and that at the RC, P_r, both measured with piezoelectric elements. Since it is important to know whether excess heat, if any, originates in nuclear effects or not, neutron and γ-ray, counting rates are monitored steadily with a ^{3}He-dosimetry counter and an NaI scintillation detector respectively. Energy spectra of γ-rays, including natural events are also recorded. All of the measured values are processed with a 'Measurement and Automation Explorer (NI-MAX)' system (National Instruments Corporation).

Calibration runs to know the heat conversion coefficient (dW/dT) and the heat recovery rate (R_h) as a function of the input power were performed using a dummy Al_2O_3 powder with an average size of 60 μm, and are described in refs 11 and 12 respectively, for the systems before and after addition of the #2 heater on the bottom flange.

H-Absorption run of the CNS sample

A series of the trial runs have been conducted to find practical problems using the system without the #2 heater. The runs used a 50-g powder of silica-included Cu·Ni nano-composite, $Cu_{0.0071}Ni_{0.030}/SiO_2$ ('CNS', Admatechs Co. Ltd), which contains 4.1 g of Ni (mostly as NiO) and 1.1 g of Cu with particle sizes of 5–50 nm in effective diameter. An energy dispersive X-ray spectrometry (EDS) photograph shows that a part of the particles contains both Cu and Ni, implying that Cu and Ni atoms are merged into single particles to form some compounds. Since the CNS sample occupied a volume of only about 200 cm^3 in the RC, a mixture of the sample with a 200 g powder of Al_2O_3, was used which is the same material as that used for the calibration/control run, to fill up the RC.

The CNS/Al_2O_3 mixture was subjected first to vacuum baking at a heater input power of 196 W for about 2 days.

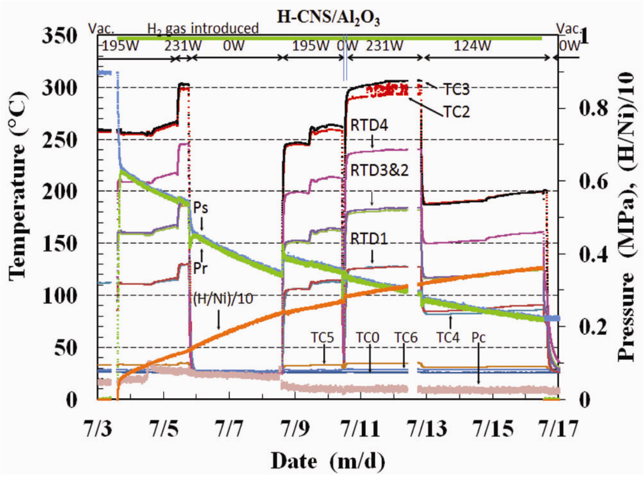

Figure 2. Temperature, pressure and loading ratio in the run H-CNS/Al$_2$O$_3$.

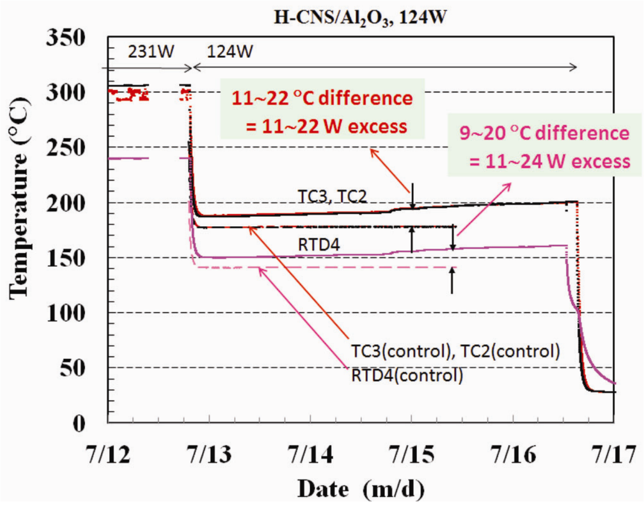

Figure 3. Comparison of temperature change during the 124 W phase in the runs H-CNS/Al$_2$O$_3$ and H-Al$_2$O$_3$.

Next we introduced the hydrogen (protium) gas into the RC, and changed the heater input power from 195 to 231, 0, 195 and 231 W again, and finally to 124 W. The whole sequence of this run, H-CNS/Al$_2$O$_3$, is shown in Figure 2, where the traces of the temperatures, TC0–TC6, except TC1 and RTD1–RTD4 are shown together with the pressures P_s, P_r and P_c at the flow-rate monitor of BT400. Moreover, the amount of hydrogen atoms lost from the gas phase is shown as (H/Ni), the ratio of the number of the hydrogen atom absorbed/adsorbed to that of the host Ni atom, i.e. the so-called loading ratio.

The parameter (H/Ni) increases almost steadily throughout the whole run, which is thought to be leakage out of the system. We also notice stepwise increases at the beginning when the gas was introduced into the RC, and just when the heater power was increased from 195 to 231 W. These should be due to real adsorption/absorption of hydrogen by the sample. Summing up the contributions, we obtain the loading ratio of 0.75 ± 0.05.

We also notice that, in contrast to the control run H-Al$_2$O$_3$ (not shown here), the temperatures increased continuously under the constant input power of 195, 231 and 124 W. Moreover, almost stepwise increases were observed for 195 and 124 W. The increase was not observed in the control run H-Al$_2$O$_3$. As an example, the temperature evolutions in the 124 W phase of the H-CNS/Al$_2$O$_3$ run were compared with those of the H-Al$_2$O$_3$ run (Figure 3). This revealed temperature increase by 11°C to 22°C at the TC2 and TC3, and by 9°C to 20°C at RTD4. If these increases are attributed to the real increases in the power, they correspond to the 'excess' powers of 11–22 W and 11–24 W respectively. When evaluated in terms of the specific power, the 'excess' amounts to 3–6 W/g-Ni.

Similar values were deduced for the temperature increases in other periods of input power. Moreover, the assumed 'excess' power was on the same order of magnitude as that claimed for the CNZ (Cu · Ni/Zi$_2$O$_3$) sample yielding an excess power of 2 W/g-Ni (ref. 13).

It is difficult to ascribe the observed temperature increase to phenomena such as decrease in the flow rate of the coolant and increase in the thermal conductivity of the sample by agglomeration of the Cu·Ni particles[11]. Instead, the observed temperature increase is likely to be caused by an excess power from the sample. It is, however, also true that the increased amount is too small to deny all other factors which could affect the temperature. We are now testing a similar silica-included sample, CNS2, with an increased amount of Ni.

H-absorption run of the CNZ4 sample

Next, absorption runs were performed on a zirconia-supported sample, a 293.6 g powder of Cu$_{0.076}$Ni$_{0.364}$/ZrO$_2$ nano-composite ('CNZ4', Santoku Corp), which contains 61.4 g (1.05 mol) of Ni and 13.8 g (0.217 mol) of Cu with crystalline diameter of 25.5 and 6.5 nm respectively. XRD measurements showed that almost all Cu and Ni atoms were oxidized. The RC was filled up by adding a 120 g powder of Al$_2$O$_3$.

The CNZ4/Al$_2$O$_3$ powder was subjected first to vacuum baking at a heater input power of up to (69 + 27) W. Two hours before introducing the H$_2$ gas to start the H-CNZ4/Al$_2$O$_3$#1 run, the heater power was adjusted to (0 + 39) W. The histories of the temperature and pressure before and after the gas introduction are shown in Figure 4.

Just after introducing the H$_2$ gas, humps were recorded in the temperatures at RTD2, RTD1 and TCs. The hump of about 10 W × 4 h at TC2 was time-integrated to give an emerging energy of 35 kJ (0.35 eV/atom-Ni). Possible mechanisms for this heat evolution are: (1) enhanced heat

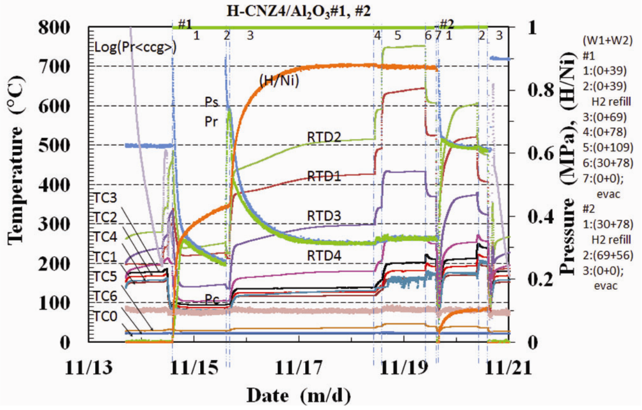

Figure 4. H-absorption runs H-CNZ4/Al_2O_3#1 followed by evacuation and H-CNZ4/Al_2O_3#2 run.

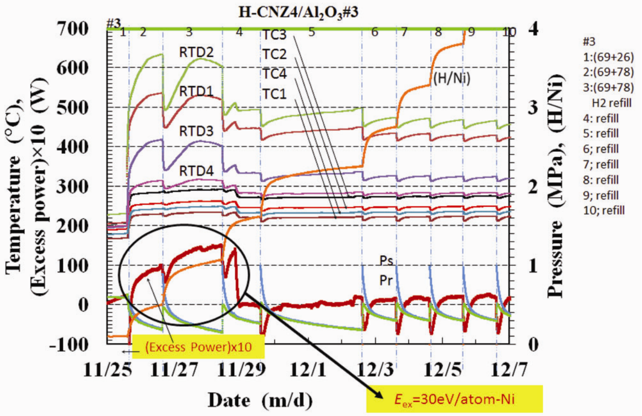

Figure 5. Excess power in the H-CNZ4/Al_2O_3#3 run. The excess is calculated as the deviation in TC2 temperature from that in the control run H-$Al_2O_3$2.

transfer effect, or transient release of the energy stored in the preceding phase in the thermally insulated sample; (2) reduction of the oxides, NiO and CuO, yielding 0.0135 eV/atom-Ni and 0.884 eV/atom-Cu respectively, and (3) hydride formation or adsorption/absorption. Since it is difficult to factor out the amount of H atoms used for the reduction reaction, it is difficult to experimentally determine the hydride formation energy, or the absorption/adsorption energy, from the present data. In the following, we discuss the excess energy mainly in the steady state, or the 'S (saturation)-phase'.

In the S-phase of #1-1, the temperatures at TC2 and TC3 have steady values, while those at RTDs and (H/Ni) are gradually increasing. When the H_2 gas was refilled at #1-2, only a small increase in (H/Ni) was observed, while (H/Ni) increased substantially, when the input power was increased at #1-3. It should be noted that the hydrogen loss did saturate at (H/Ni) ~ 0.9, which remained even when the power was increased further in #1-4 through #1-6. After an evacuation phase #1-7 at some elevated temperature, the #2 run was started with #2-1 phase, where the loss (H/Ni) did not grow above 0.1. Even in the #3 run after more elaborate baking for two days, the hydrogen loss remained at (H/Ni) ~ 0.1.

These facts imply the following: (a) It is natural to attribute (H/Ni) ~ 0.1 in the #2 run to absorption/adsorption by the sample. (b) The difference of the loss in #1-3 through #1-6 and that in #2-1, (H/Ni) ~ 0.8, should correspond to the number of H atoms necessary for the reduction reaction. (c) Temperature of about 180°C is necessary for the reduction reaction to proceed, and is sufficient for absorption/adsorption to proceed. (d) There was no leakage of gas out of the system at least at this stage of the runs.

The value of (H/Ni) remained modest in the #3–1 phase, as shown in Figure 5. However, (H/Ni) suddenly grew to about 0.5 at the beginning of the #3-2 phase, when the heater power was increased to (69+78) W. H_2 gas refill was repeated thereafter.

Looking at the temperatures in the phases #3-2 through #3-4, we notice long-term humps in the RTDs and TCs. If we take the base (zero-power) line for TC2 as the temperature at TC2 in the case of calibration/control, we can express the excess power as a function of time, which is shown in Figure 5 as the thick red line, where the excess power is multiplied by 10 for viewability.

The excess grew to the maximum value of 15 W (0.25 W/g-Ni), and was quenched suddenly at midnight on 28 November, forming an 80 h hump. Integrating the power, we obtained excess energy of 3 MJ/mol-Ni (30 eV/atom-Ni). This is several to ten times larger than the energy generated by any chemical reaction. If we assume that the increase in (H/Ni) (~1.5) during this 80 h period was entirely related to the excess phenomenon, the excess energy is expressed as 20 eV/atom-H at least. This is more than one order of magnitude larger than the energy produced in, for example, the water-producing reaction: $H_2 + (1/2)O_2 \rightarrow H_2O + 2.97$ eV. It is inferred that a nuclear process is involved.

The excess was retrieved. Beginning on 2 December the excess power of several watts gradually increased to 10 W (0.17 W/g-Ni) 3 weeks later, which gives an integrated energy of 10 MJ/mol-Ni (100 eV/atom-Ni).

The above values of the excess power of the order of 10 W (10^{-1} W/g-Ni) are one order of magnitude smaller than that expected for the present sample of CNZ4. They are one order of magnitude smaller than that claimed for the CNZ sample yielding an excess power of 2 W/g-Ni using the $A_1 \cdot A_2$ system[6]. We still need one order of magnitude larger temperature change to claim excess heat with absolute certainty. Nevertheless, it is also true that it is difficult to find a reasonable cause other than excess heat for the temperature change at the present stage.

Now we discuss the stepwise increase in (H/Ni) accompanied by the negative spikes in the temperature observed in every phase of gas refill. The stepwise increase Δ(H/Ni) ~ 0.5 corresponds to a loss of 0.25-mol H_2, while the negative spike in temperature corresponds to a lost/absorbed energy of the order of 0.01 eV per one atom contained in the system, or to 1.3 eV/atom-Ni, or to 2.6 eV/atom-H, if only Ni/H atoms are assumed to be concerned in the loss/absorption.

These values are not very large as a chemical reaction energy, while they are too large as a gas-dynamical reaction energy or even as the adsorption/absorption energy. The negative energy introduced to the hot (~300°C) system by supplying the H_2 gas at room temperature, 0.025 eV/H_2, is more than two orders of magnitude smaller than the value 2.6 eV/atom-H.

We now know that there had been some leak of H_2 gas from the system detected by a hydrogen leak checker. However, the leak cannot be the major origin of the endotherm of 2.6 eV/atom-H, since the thermal energy of the H_2 molecule at 300°C, 0.05 eV/H_2, is again two orders of magnitude smaller. Further study is necessary to solve this paradox of absorbed energy.

Finally, we have to mention that any noticeable change both in the γ-ray and the neutron counting rates was not coincident with the excess power evolution.

1. Celani, F. *et al.*, Cu–Ni–Mn alloy wires, with improved sub-micrometric surfaces, used as LENR device by new transparent, dissipation-type, calorimeter. *J. Condens. Matter Nucl. Sci.*, 2014, **13**, 56–67.
2. Piantelli, F., Nichenergy; http://e-catsite.com/2012/06/15/piantelli-moves-closer-to-commercialization/
3. Rossi, A., Leonardo Corp., http://ecat.com
4. Hadjichristos, J., Defkalion Green Technol., http://www.youtube.com/watch?v=J006idrZEcw
5. Kitamura, A., Sasaki, Y., Miyoshi, Y., Taniike, A., Takahashi, A., Seto, R. and Fujita, Y., Heat evolution from Pd nanopowders exposed to high-pressure hydrogen isotopes and associated radiation measurements. *J. Condens. Matter Nucl. Sci.*, 2011, **4**, 56–68.
6. Miyoshi, Y., Sakoh, H., Taniike, A., Kitamura, A., Takahashi, A., Seto, R. and Fujita, Y., Effect of forced oxidation on hydrogen isotope absorption/adsorption characteristics of Pd·Ni·Zr oxide compounds. *J. Condens. Matter Nucl. Sci.*, 2013, **10**, 46–62.
7. Kitamura, A., Nohmi, T., Sasaki, Y., Taniike, A., Takahashi, A., Seto, R. and Fujita, Y., Anomalous effects in charging of Pd powders with high density hydrogen isotopes. *Phys. Lett. A*, 2009, **373**, 3109–3112.
8. Miyoshi, Y., Sakoh, H., Taniike, A., Kitamura, A., Takahashi, A., Seto R. and Fujita, Y., Gas-phase hydrogen isotope absorption/adsorption characteristics of a Ni based sample. In Proceedings of JCF12, 2012, pp. 1–9.
9. Sakoh, H. *et al.*, Hydrogen isotope absorption and heat release characteristics of a Ni-based sample. *J. Condens. Matter Nucl. Sci.*, 2014, **13**, 471–484.
10. Sakoh, H. *et al.*, Heat release characteristics of Ni-based samples absorbing hydrogen isotopes at high temperature. In Proceedings of JCF13, 2013, pp. 214–229.
11. Kitamura, A., Takahashi, A., Seto, R., Fujita, Y., Taniike, A. and Furuyama, Y., Mass-flow-calorimetry system for scaled-up experiments on anomalous heat evolution at elevated temperatures; https://mospace.umsystem.edu/xmlui/handle/10355/36813
12. Kitamura, A., Takahashi, A., Seto, R., Fujita, Y., Taniike, A. and Furuyama, Y., Study on anomalous heat evolution from H–Ni nanoparticle system at elevated temperature with mass–flow calorimetry. In Proceedings of JCF14, 2014, pp. 1–13.
13. Takahashi, A. *et al.*, Anomalous exothermic and endothermic data observed by nano-Ni-composite samples; https://mospace.umsystem.edu/xmlui/handle/10355/36494